RAPID COMMUNICATIONS

PHYSICAL REVIEW B VOLUME 47, NUMBER 14 1 APRIL 1993-II

Evidence for $d_{x^2-y^2}$ pairing from nuclear-magnetic-resonance experiments in the superconducting state of $YBa_2Cu_3O_7$

D. Thelen and D. Pines
Physics Department, University of Illinois at Urbana-Champaign, 1110 West Green Street, Urbana, Illinois 61801

Jian Ping Lu
Department of Physics and Astronomy, University of North Carolina at Chapel Hill, CB 3255, Chapel Hill, North Carolina 27599
(Received 29 December 1992)

We calculate the electron spin susceptibility for the superconducting state of $YBa_2Cu_3O_7$ using a band structure with nearest- and next-nearest-neighbor hopping, a momentum-dependent spin-spin interaction, and a superconducting gap with $d_{x^2-y^2}$ symmetry. Our calculated nuclear magnetic relaxation rates and Knight shift agree favorably with experiment. Our work provides further evidence for a $d_{x^2-y^2}$ pairing state and demonstrates that antiferromagnetic correlations persist in the superconducting state.

While it is commonly accepted that BCS theory provides a framework for analyzing the superconducting properties of the cuprates, no clear consensus has emerged on the nature of the pairing state. This is of central importance in determining the mechanism for high-temperature superconductivity. For example, the recent strong-coupling calculations of Monthoux and Pines[1] for $YBa_2Cu_3O_7$ which demonstrate that a spin-fluctuation-induced interaction can yield a high T_c, require that the pairing state be $d_{x^2-y^2}$. NMR experiments offer considerable promise in resolving this issue because they probe the structure in momentum space of the electron spin susceptibility $\chi(q,\omega)$; the latter is in turn sensitive to the band structure, interactions, and lifetime in the normal state, and to the superconducting gap in the superconducting state.

Recent experiments on the ^{63}Cu spin-lattice relaxation rate of $YBa_2Cu_3O_7$ show that its temperature dependence is different for magnetic fields applied perpendicular and parallel to the Cu-O planes[2] while for the same direction of applied field, the temperature dependence of the ^{63}Cu and ^{17}O relaxation rates is also quite different.[3] Together with earlier Knight shift experiments[4] these rule out s-wave pairing and provide strong constraints on any other candidate theory. Thus while Monien and Pines[5] could fit nuclear-quadrupole-resonance (NQR) and Knight shift experiments reasonably well with d-wave pairing and strong-coupling gap parameters, and Bulut and Scalapino[6] and Lu[7] could explain the temperature-dependent anisotropy of the ^{63}Cu relaxation rate by using a quasiparticle spectrum with nearest-neighbor hopping in a random-phase-approximation (RPA) calculation in which the effective spin-spin interaction was momentum independent, neither approach was capable of explaining the ^{17}O relaxation rate. We show below that when the quasiparticle spectrum includes next-nearest-neighbor hopping, the effective interaction is taken to be momentum dependent (with the same momentum dependence as that required to explain the normal-state NMR experiments), and lifetime effects of the magnitude measured by Bonn *et al.*[8] are taken into account, good quantitative agreement with experiment is found provided the pairing state is $d_{x^2-y^2}$.

The nuclear magnetic relaxation rate W of a nuclear site α and direction of static applied field γ is related to $\chi(\mathbf{q},\omega)$ by

$$^{\alpha}W_{\gamma}=\frac{3k_bT}{4\mu_b^2\hbar}\lim_{\omega\to 0}\sum_q {}^{\alpha}F_{\gamma}(q)\frac{\mathrm{Im}\chi(\mathbf{q},\omega)}{\hbar\omega}\ , \tag{1}$$

where the hyperfine form factors $^{\alpha}F_{\gamma}(q)$ have been determined by Mila and Rice[9] to be

$$^{63}F_{\parallel}=\{A_{\perp}+2B[\cos(q_xa)+\cos(q_ya)]\}^2\ , \tag{2}$$

$$^{63}F_{\perp}=\tfrac{1}{2}\{A_{\parallel}+2B[\cos(q_xa)+\cos(q_ya)]\}^2 + \tfrac{1}{2}\{A_{\perp}+2B[\cos(q_xa)+\cos(q_ya)]\}^2\ , \tag{3}$$

$$^{17}F_{\parallel}=2C^2\{1+\tfrac{1}{2}[\cos(q_xa)+\cos(q_ya)]\}\ . \tag{4}$$

The difference between $^{63}F_{\parallel}$ and $^{63}F_{\perp}$ is brought out more clearly by defining another form factor, $^{63}F_{\perp}^{\mathrm{eff}}$,

$$^{63}F_{\perp}^{\mathrm{eff}}=\{A_{\parallel}+2B[\cos(q_xa)+\cos(q_ya)]\}^2 \tag{5}$$

and a corresponding relaxation rate $^{63}W_{\perp}^{\mathrm{eff}}$

$$^{63}W_{\perp}^{\mathrm{eff}}=2\,{}^{63}W_{\perp}-{}^{63}W_{\parallel}\ . \tag{6}$$

We take $A_{\parallel}=-4B$, $A_{\perp}=0.84B$, and $C=0.91B$. The resulting independent form factors $^{17}F_{\parallel}$, $^{63}F_{\parallel}$, and $^{63}F_{\perp}^{\mathrm{eff}}$, shown in Fig. 1, explain the difference between rates at different sites. Thus the oxygen rate is unaffected by what is happening at the antiferromagnetic wave vector, while the effective copper rate perpendicular to c has no weight near $q=0$, but has a large weight near $(\pi/a,\pi/a)$. The copper rate parallel to c is the most complicated be-

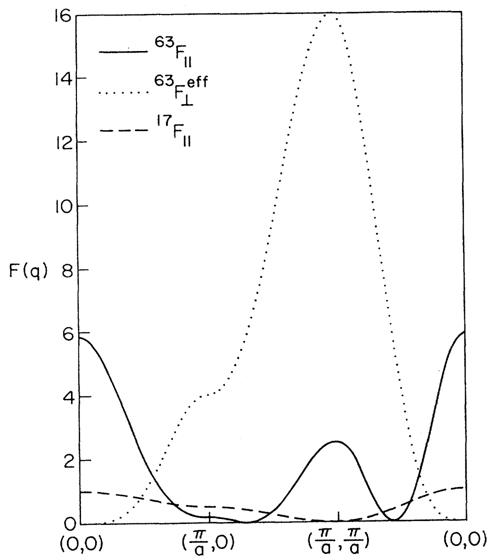

FIG. 1. Form factors as a function of momentum for oxygen $^{17}F_{\parallel}$ in units of C^2 and for copper sites $^{63}F_{\perp}^{\mathrm{eff}}$ and $^{63}F_{\parallel}$ in units of $4B^2$.

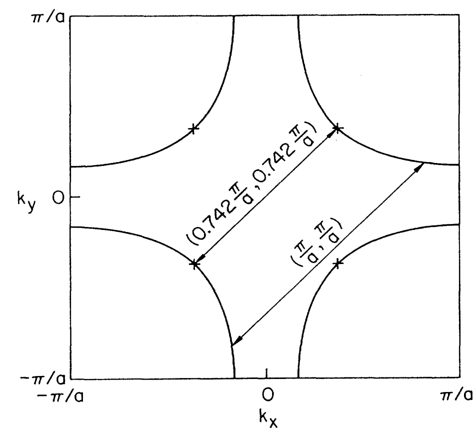

FIG. 2. Fermi surface for $t'=-0.45t$. The + symbols indicate nodes on the Fermi surface for a $d_{x^2-y^2}$ superconductor, connected by momenta $(0.742\pi/a, 0.742\pi/a)$.

cause the form factor vanishes at values of momentum which are determined by the ratio of $A_{\perp}$ to B.

We assume that $\chi(\mathbf{q},\omega)$ takes the RPA form,

$$\chi(\mathbf{q},\omega)=\frac{\tilde{\chi}(\mathbf{q},\omega)}{1-J(\mathbf{q})\tilde{\chi}(\mathbf{q},\omega)}, \tag{7}$$

where the irreducible susceptibility, $\tilde{\chi}(\mathbf{q},\omega)$, will depend in the normal state on the quasiparticle spectrum and lifetime effects, and in the superconducting state, on the pairing state and gap parameters. We take the same quasiparticle spectrum as that employed by Monthoux and Pines[1],

$$\varepsilon_{\mathbf{k}}=-2t[\cos(k_x)+\cos(k_y)]-4t'\cos(k_x)\cos(k_y)-\mu, \tag{8}$$

where t and t' are nearest-neighbor and next-nearest-neighbor hopping and μ is the chemical potential. This band structure differs significantly from that used in previous calculations of NMR relaxation rates[6,7] which used $t'=0$. We take $t'=-0.45t$, set $t=0.25$ eV (corresponding to a bandwidth of $8t=2$ eV), and use $k_f=(0.371,0.371)\pi/a$ to determine the chemical potential. This choice of parameters yields a Fermi surface, shown in Fig. 2, close to that measured in photoemission experiments.[10] Note that the antiferromagnetic wave vector $(\pi/a,\pi/a)$ spans the Fermi surface while the wave vectors which connect nodes of the superconducting gap on the Fermi surface are significantly away from $(\pi/a,\pi/a)$.

We choose the momentum-dependent interaction, $J(\mathbf{q})$, in such a way that Eq. (7) yields a quantitative account of the ^{63}Cu and ^{17}O NMR relaxation rates just above T_c when we take for $\tilde{\chi}(\mathbf{q},\omega)$ the strong-coupling value calculated by Monthoux and Pines;[1] we take it to be[11]

$$J(\mathbf{q})=J_0-2J[\cos(q_xa)+\cos(q_ya)]-4J'\cos(q_xa)\cos(q_ya)-2J''[\cos(2q_xa)+\cos(2q_ya)] \tag{9}$$

with $J_0=0.347$ eV, $J=2.73\times10^{-2}$ eV, and $J'=J''=-0.9J$. We assume that $J(\mathbf{q})$ is unchanged in the superconducting state.

Strong-coupling calculations of $\tilde{\chi}(\mathbf{q},\omega)$ in the superconducting state have not yet been carried out; we assume that these may be approximated by reducing the noninteracting susceptibility, $\mathrm{Re}[\chi_0(\mathbf{q},\omega)]$ by some 0.58, this being the reduction factor which provides a quantitative fit to the results of Monthoux and Pines near T_c; thus we take $\mathrm{Re}[\tilde{\chi}(\mathbf{q},\omega)]\approx\mathrm{Re}[\tilde{\chi}(\mathbf{q},0)=0.58\mathrm{Re}(\chi_0(\mathbf{q},0))]$ and calculate $\chi_0(\mathbf{q},0)$ from the BCS expression

$$\chi_0(\mathbf{q},\omega)=\sum_k\left[1+\frac{\varepsilon_{\mathbf{k}+\mathbf{q}}\varepsilon_{\mathbf{k}}+\Delta_{\mathbf{k}+\mathbf{q}}\Delta_{\mathbf{k}}}{E_{\mathbf{k}+\mathbf{q}}E_{\mathbf{k}}}\right]\frac{f(E_{\mathbf{k}+\mathbf{q}})-f(E_{\mathbf{k}})}{\omega-(E_{\mathbf{k}+\mathbf{q}}-E_{\mathbf{k}})+i\Gamma}+\frac{1}{2}\left[1-\frac{\varepsilon_{\mathbf{k}+\mathbf{q}}\varepsilon_{\mathbf{k}}+\Delta_{\mathbf{k}+\mathbf{q}}\Delta_{\mathbf{k}}}{E_{\mathbf{k}+\mathbf{q}}E_{\mathbf{k}}}\right]\frac{1-f(E_{\mathbf{k}+\mathbf{q}})-f(E_{\mathbf{k}})}{\omega+(E_{\mathbf{k}+\mathbf{q}}+E_{\mathbf{k}})+i\Gamma}+\frac{1}{2}\left[1-\frac{\varepsilon_{\mathbf{k}+\mathbf{q}}\varepsilon_{\mathbf{k}}+\Delta_{\mathbf{k}+\mathbf{q}}\Delta_{\mathbf{k}}}{E_{\mathbf{k}+\mathbf{q}}E_{\mathbf{k}}}\right]\frac{f(E_{\mathbf{k}+\mathbf{q}})+f(E_{\mathbf{k}})-1}{\omega-(E_{\mathbf{k}+\mathbf{q}}+E_{\mathbf{k}})+i\Gamma}, \tag{10}$$

where $\varepsilon_{\mathbf{k}}$ and $\Delta_{\mathbf{k}}$ are band and gap functions, respectively. $E_{\mathbf{k}}$ is defined as $\sqrt{\varepsilon_{\mathbf{k}}^2+\Delta_{\mathbf{k}}^2}$. $f(E)$ is the Fermi function and Γ is the scattering rate. We choose

$$\Gamma=(0.59e^{(T-T_c)/14.1K}+.01)k_bT_c \tag{11}$$

to agree with the measurements of Bonn *et al.*;[8] at $T_c=93$ K, the scattering rate is $2\Gamma=1.2k_bT_c$. The constant term $0.01k_bT_c$ is chosen to give a reasonable rate for the copper relaxation rate at low temperature; it only has a significant effect at low temperature. Near $q=0$ we

RAPID COMMUNICATIONS

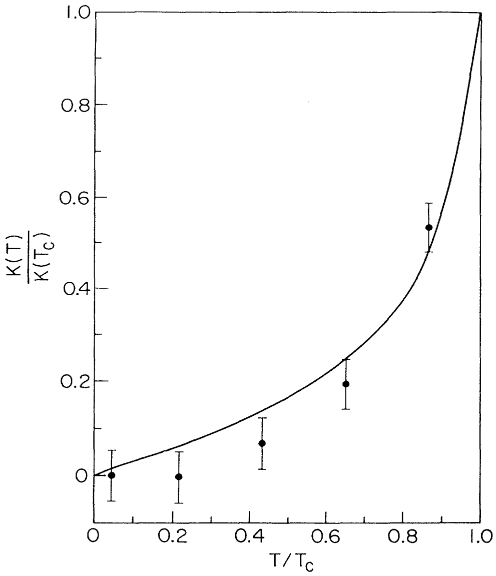

FIG. 3. A comparison of our calculated Knight shift, denoted by a solid line, with the experimental data of Barrett *et al.* (Ref. 4).

introduce a form factor which reduces Γ to zero so that the quasiparticles are well defined. The resulting commensurate imaginary susceptibility at T_c has a height and dispersion near $(\pi/a,\pi/a)$ which corresponds to a correlation length in the theory of Millis, Monien, and Pines[12] of 2.3 lattice spacings and a β of 9.9, the same values as those found in the analysis of the $YBa_2Cu_3O_7$ materials.[13]

For the $d_{x^2-y^2}$ pairing state the gap function may be written as

$$\Delta_k = \Delta(T)[\cos(k_x) - \cos(k_y)] \ . \tag{12}$$

We parametrize $\Delta(T)$ as

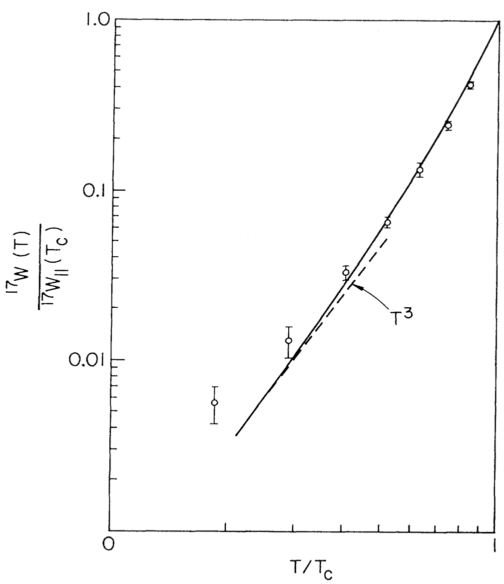

FIG. 4. A comparison of our calculated oxygen relaxation rate, denoted by a solid line, with the experimental data of Martindale *et al.* (Ref. 3).

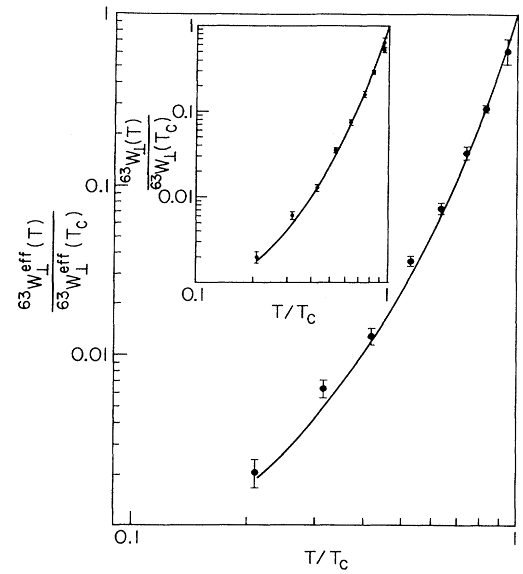

FIG. 5. A comparison of our calculated effective copper rate perpendicular to c, denoted by a solid line, with the experimental data of Martindale *et al.* (Ref. 2). Inset: A comparison of the calculated copper rate perpendicular to c, denoted by a solid line, with the experimental data of Martindale *et al.* (Ref. 2).

$$\Delta(T) = \Delta(0)\tanh(\alpha\sqrt{T_c/T - 1}) \tag{13}$$

and choose the maximum value of the gap in the Brillouin zone to be $3k_bT_c$ [which determines $\Delta(0)$] and $\alpha = 2.2$ in order to obtain agreement with the Knight shift experiments of Barrett *et al.*[4] Our calculated

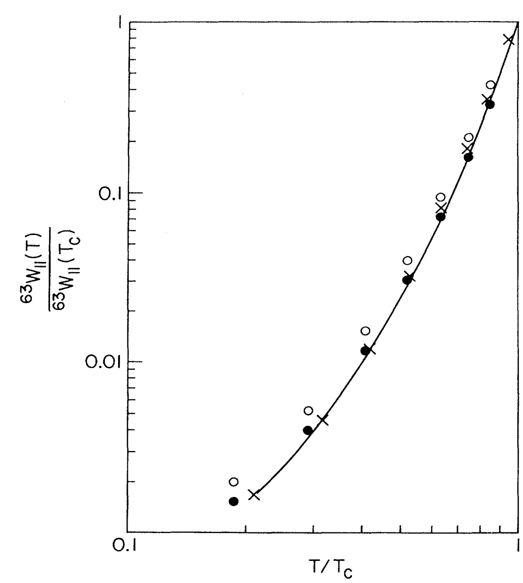

FIG. 6. A comparison of our calculated copper rate parallel to c, denoted by a solid line, with the experimental data for two samples measured by Martindale *et al.* Crosses denote data from Ref. 2; open circles indicate data from Ref. 3; filled circles indicate data from Ref. 3, restated to reflect the possibility that $^{63}W_{\parallel}(T_c) = 1.064$ m s^1, a value which makes possible a more consistent picture of the ^{63}Cu relaxation rate in the vicinity of T_c for this sample.

Knight shift normalized to T_c is compared to the experimental data of Barrett *et al.*[4] in Fig. 3.

Our calculated ^{17}O relaxation rate is compared to the measured[3] low-field oxygen rate (normalized to T_c) in Fig. 4. Note the absence of a Hebel-Slichter coherence peak, the development of a T^3 term in the rate at low temperature which reflects the presence of a line of nodes in the gap, and the close agreement between theory and experiment. The calculated and measured effective copper relaxation rates for an external field perpendicular to c are shown in Fig. 5, while the corresponding relaxation rates for an external field parallel to the c axis are shown in Fig. 6. Since both form factors are sensitive to the degree of antiferromagnetic enhancement, and the latter is reduced in the superconducting state once internodal scattering predominates, there is no significant T^3 region in either relaxation rate. Both our theoretical calculations and the experimental data for the copper rate anisotropy show that it decreases and then rises as one enters the superconducting state. The effective copper rate perpendicular to c decays more rapidly than the oxygen rate because the imaginary part of the susceptibility near $(\pi/a,\pi/a)$ effectively becomes gapped as one enters the superconducting state. Previous calculations[6,7] with a $t'=0$ band structure did not find a significant falloff in the copper to oxygen ratio as one enters the superconducting state; with the value $t'=-0.45t$ used here, the small copper to oxygen ratio is produced by the nodes of the gap on the Fermi surface. In the normal state, the imaginary part of the susceptibility is peaked at the antiferromagnetic wave vector $(\pi/a,\pi/a)$; this gives a large copper to oxygen rate ratio [due to the cancellation of the oxygen form factor at $(\pi/a,\pi/a)$]. As the gap opens, the susceptibility becomes peaked away from $(\pi/a,\pi/a)$ but near wave vectors which connect nodes on the Fermi surface. Since this increases the oxygen rate relative to the copper, the copper to oxygen rate ratio decreases.

Our calculation of the susceptibility gives good agreement with all three experimentally observed relaxation rates. While the calculations performed here are no substitute for a fully self-consistent calculation in the superconducting state, they demonstrate that when proper account is taken of band-structure, strong-coupling, and lifetime effects, the interplay between antiferromagnetic correlations and the $d_{x^2-y^2}$ symmetry of the superconducting order parameter gives rise to the experimentally determined relaxation rates.

We would like to thank C. P. Slichter, J. Martindale, and S. Barrett for many helpful discussions and for data in advance of publication, and J. Annett, N. Bulut, N. Goldenfeld, L. P. Gorkov, P. Monthoux, J. J. Yu and many others for useful discussions. This work was supported by the Science and Technology Center for Superconductivity under NSF Grant No. DMR91-20000. The calculations were performed on the Cray YMP at the National Center for Supercomputing Applications at the University of Illinois at Urbana-Champaign.

[1]P. Monthoux and D. Pines, Phys. Rev. Lett. **69**, 961 (1992); Phys. Rev. B **47**, 6069 (1993).
[2]J. A. Martindale *et al.*, Phys. Rev. Lett. **68**, 702 (1992).
[3]J. Martindale *et al.*, following paper, Phys. Rev. B **47**, 9155 (1993).
[4]S. Barrett *et al.*, Phys. Rev. B **41**, 6283 (1990).
[5]H. Monien and D. Pines, Phys. Rev. B **41**, 6297 (1990).
[6]N. Bulut and D. J. Scalapino, Phys. Lett. **68**, 706 (1992).
[7]J. P. Lu, Mod. Phys. Lett. B **6**, 547 (1992).
[8]D. A. Bonn *et al.*, Phys. Rev. Lett. **68**, 2390 (1992); D. A. Bonn *et al.* (unpublished).
[9]F. Mila and T. M. Rice, Physica (Amsterdam) **157C**, 561 (1989).
[10]J. C. Campuzano *et al.*, Phys. Rev. Lett. **64**, 2308 (1990).
[11]D. Thelen, P. Monthoux, and D. Pines (unpublished).
[12]A. J. Millis, H. Monien, and D. Pines, Phys. Rev. B **42**, 167 (1990).
[13]H. Monien, D. Pines, and M. Takigawa, Phys. Rev. B **43**, 258 (1991).